IEEE Access
Multidisciplinary ⋮ Rapid Review ⋮ Open Access Journal

Received March 22, 2022, accepted April 18, 2022, date of publication April 22, 2022, date of current version May 3, 2022.

Digital Object Identifier 10.1109/ACCESS.2022.3169791

Control of PV Systems for Multimachine Power System Stability Improvement

YANDI G. LANDERA[1], OSCAR C. ZEVALLOS[2], (Member, IEEE), FRANCISCO A. S. NEVES[1], (Senior Member, IEEE), RAFAEL C. NETO[1], (Student Member, IEEE), AND RICARDO B. PRADA[2]

[1]Power Electronics and Drives Research Group (GEPAE), DEE, Universidade Federal de Pernambuco, Recife 50740-530, Brazil
[2]Department of Electrical Engineering, Pontifical Catholic University of Rio de Janeiro, Rio de Janeiro 22451-900, Brazil

Corresponding author: Yandi G. Landera (yandi.gallego@ufpe.br)

This work was supported in part by the Brazilian National Council for Scientific and Technological Development (CNPq) under Grant 307966/2018-6, and in part by the Brazilian National Coordination for the Improvement of Higher Education Personnel (CAPES).

ABSTRACT The goal of achieving decarbonized operation of power systems in response to climate change has led to an increase in the number of sources connected to electrical grids through inverters, of which photovoltaic systems are an example. The operating characteristics of these systems in steady-state or transient operation are different from those of synchronous machines, giving rise to issues related to power system stability. The vast majority of grid codes stipulate that fault ride-through operating requirements should be enabled during severe contingencies in the transmission network, prioritizing delivery of reactive power to the power system to support voltage stability. However, this control action may contribute to rapid collapse of the system voltage under adverse operating conditions, such as when the critical voltage in the power vs. voltage curve is near the reliable voltage operating bound. Supporting power system stability under these circumstances represents a new challenge for inverter control schemes. This paper adapts a recently published fault ride-through control scheme for PV inverters for use in a multimachine power system and shows that the scheme can successfully maintain transient and voltage stability even under adverse voltage operating conditions.

INDEX TERMS Fault ride-through, grid code, multimachine power system, photovoltaic generation, transient stability, voltage stability.

NOMENCLATURE

C_f	Inverter shunt filter capacitance.
$i_{abc}^{TL\text{-}k}$	k-transmission line current in abc reference frame.
$i_{g,abc}$	Grid current in abc reference frame.
$i_{PMU}^{TL\text{-}k}$	PMU's k-transmission line current measurement.
$i_{PV,abc}$	PV power system current in abc reference frame.
$i_{SM,abc}$	Synchronous machine current in abc reference frame.
L_f	Inverter series filter inductance.
n	Number of PV units.
p^*	Reference instantaneous active power.
$\overline{P}_g^f$	Grid average active power during fault.
P_{inv}^*	Inverter reference active power.
$P, Q_{TL\text{-}k}^{pre\text{-}f}$	k-transmission line pre-fault active and reactive power.
$P, Q_{TL\text{-}k}^{f}$	k-transmission line active and reactive power during fault.
$\overline{P, Q}_{TL\text{-}k}^{f}$	k-transmission line average active and reactive power during fault.
P_{max}^{inv}	Inverter maximum active power.
p_{mppt}^*	MPPT inverter reference active power.
$P, Q_{PV\text{-}k}^*$	PV system reference active and reactive power of the k-transmission line.
P, Q_{PV}^*	PV system reference active and reactive power.
$P_{SM}^{pre\text{-}f}$	Synchronous machine pre-fault active power.
q^*	Reference instantaneous reactive power.

The associate editor coordinating the review of this manuscript and approving it for publication was N. Prabaharan.

$\overline{Q}_{g}^{f}$	Grid average reactive power during fault.
Q_{inv}^{*}	Inverter reference reactive power.
Q_{max}^{inv}	Inverter maximum reactive power.
q_{mppt}^{*}	MPPT inverter reference reactive power.
$Q_{SM}^{pre\text{-}f}$	Synchronous machine pre-fault reactive power.
R_f	Inverter series filter resistor.
S_{max}^{inv}	Inverter maximum apparent power.
TL-f	Transmission line subjected to a fault.
v_{abc}^{PCC}	PCC voltage in abc reference frame.
v_{PMU}^{PCC}	PMU's PCC voltage measurement.
δ	SM rotor angle.

ABBREVIATIONS

APRRR	Active power recovery ramp rate.
dc	Direct current.
FD	Fault detection.
FFPS	Fundamental frequency positive sequence.
FRT	Fault ride-through.
GC	Grid code.
IEC	International Electrotechnical Commission.
LPF	Low-pass filter.
MAF	Moving average filter.
MPPT	Maximum power point tracking.
PCC	Point of common coupling.
PDC	Phasor data concentrator.
PV	Photovoltaic.
PMU	Phasor measurement unit.
RES	Renewable energy sources.
SM	Synchronous machine.
WSCC	Western System Coordinating Council.

I. INTRODUCTION

The negative environmental impact of burning fossil fuels for energy conversion, a process which releases enormous amounts of carbon dioxide and other greenhouse gases into the atmosphere [1], [2], has focused attention on the use of renewable energy sources (RES) to generate electricity. In general, conventional fossil fuels are non-renewable, posing a potential threat of resource depletion. The most advanced RES that has been widely integrated with electrical grids and represents a trend in modern energy systems is photovoltaic solar energy [3], considered one of the most vital and promising RES [4].

The current higher levels of penetration of photovoltaic (PV) Power Plants in electrical networks have made them a possible cause of stability and reliability problems when they are disconnected from the network during severe faults [5], [6]. In an attempt to solve these problems, several countries and major international organizations, such as the IEEE in the United States and the International Electrotechnical Commission (IEC) in Switzerland, have imposed and updated various standards, requirements and regulations for the operation of RES [7]–[10], particularly PV systems. These are known as grid code (GC). GCs contain a variety of technical specifications describing important rules and restrictions associated with renewable energy generating units and their integration into the electrical grid to ensure stable, correct operation of the electrical system [11] and that PV plants remain connected to the grid in the event of a grid failure, a capability known as fault ride-through (FRT). A FRT capability ensures that the PV inverter behaves like traditional synchronous generators and tolerates voltage drops resulting from faults or disturbances in the grid, remains connected to the grid and delivers or absorbs the amount of reactive power specified by the GC during the disturbance [12]. Among the countries that have reviewed and updated the requirements for PVs in their network codes, the following stand out:

- Germany, one of the leading countries in this field, imposed two GCs in 2008 that address the high penetration of RES such as wind and PV [10], [13]. The requirements specified in these GCs have served as a reference for the development of codes in other countries and for the integration of other RES in grids. In January 2015, the German GC stipulated all renewable energy plants should be able to contribute dynamic support to the grid [14];
- Spain, like Germany, is adopting new requirements in its GC [8], [9];
- Italy adopted a new version of their GC for distributed generation systems, including PV generation in the CEI 0-16, (2012) and CEI 0-21, (2014) standards, which were recently updated [15];
- The United States implemented new PV integration requirements beginning in 2003 with the IEEE standard [16], which was reviewed and updated in 2018 [17];
- The most recent GC in Australia introduced the requirements stipulated in AS4777, which follows the National Electricity Rules [18];
- Other countries have also revised their GCs for the interconnection of RES, such as Denmark [19], China [20] and Ireland [21]. Also of relevance is the European standard IEC 61727 [22].

In the last decade, GCs for the integration of PV energy [23], global standards for interconnection of RES [24], wind system regulations [25], integration of other RES [26] and standards for microgrids [27], [28] have been the subject of various studies. In [12] a brief comparison was made of the requirements for regulating voltage and frequency behavior during disturbances in the grid implemented by Germany, the United States, Italy and Australia. In 2009, a general review was published [29] which focused on European transmission system operators, US Federal Energy Regulatory Commission standards and operators in Canada and New Zealand. Similarly, another study [30] reviewed and studied German and Spanish GCs in relation to the penetration of wind energy in the electricity grid, while in [31] the GCs of North Africa and Spain were compared. In [32], the authors presented a thorough overview of voltage,

frequency and active and reactive power regulation in GCs in Germany, Romania, the United States, China, South Africa and Puerto Rico.

Some important studies have been published on the integration of RES and the proposed control strategies to act during network faults. A study published in 2019 [33] reviewed the inertial and frequency control strategies in power systems with a high penetration of RES, particularly wind and PV. However, the requirements imposed by different GCs are not addressed in the study.

In 2021, an FRT control scheme [34] based on absorption of the kinetic energy stored in the rotating mass of the synchronous machine (SM) to guarantee transient stability was proposed. The proposed control scheme also improves voltage stability by delivering reactive power to the grid, leading to rapid post-fault voltage recovery. Essentially, the active power output of the SM is kept close to its pre-fault value, and there is a significant reduction in rotor angle deviations within the first cycles of the disturbance. However, the electrical system configuration used to implement the proposed control scheme only considers a single position for the PV plant, between the grid and the SM. The electrical system consists of a single machine connected to an infinite bus, with the PV system connected in parallel to the machine. No tests were carried out on a meshed power system with several SMs in operation.

The present study aims to assess the performance of the control scheme proposed in [34] when used in a meshed power system. The results are compared with those obtained when the requirements of the German GC are met [14]. Both strategies are used to control the inverters of a PV system in a modified Western System Coordinating Council (WSCC) 9-bus power system [35] during a major disturbance in the transmission network. The paper focuses on making the necessary adjustments to the control scheme proposed in [34] and shows that the scheme can be adapted to be applied in a meshed power system under the stresses of a severe fault and helps to significantly improve the transient and voltage stability of the power system.

The paper is structured as follows: Section II introduces the proposed control scheme of the PV inverters adapted for use in a meshed power system. Section III describes the current challenges that a power system faces when RES are connected to the grid through inverters and how future FRT schemes could be modelled to support power system stability. Section IV compares and discusses the results of simulation of the test system with the proposed control scheme and with the control as required by the German GC. Finally, the conclusions are summarized in Section V.

II. PROPOSED FRT CONTROL SCHEME FOR PV INVERTERS IN A MULTIMACHINE POWER SYSTEM

The FRT control scheme proposed in [34] for a single SM and single PV system connected to a power system was modified in this paper to allow the control scheme to work in a meshed electrical system operating with several SMs, loads and transmission lines.

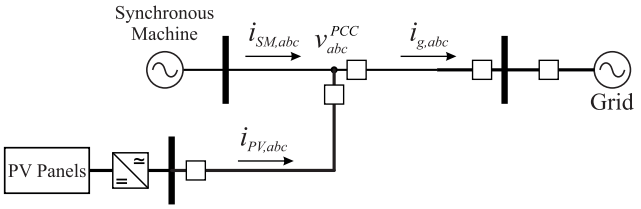

FIGURE 1. Radial power system used to design the control scheme in [34].

The main objective of the FRT control scheme in [34] is to keep the active power output of the SM at the pre-fault value during a major disturbance in the transmission system. For this to be achieved, during the fault the kinetic energy stored in the rotating mass of the SM is absorbed into the PV system's dc-link capacitors. The capacity to absorb energy is limited by the inverter's maximum direct current (dc) bus voltage [36]. This limit imposes a maximum active power that can be absorbed by the dc-link capacitors, leaving a portion of power available that can be dispatched in the form of reactive power as required by some GCs [14]. The control scheme has two major advantages: it supports operation of the electrical system by improving both transient and voltage stability during a major disturbance. In contrast, most GCs only require that voltage stability be supported. However, the control scheme was conceived considering a radial power system with a single SM connected to an infinite bus through a transmission network and the PV system connected to the grid in parallel to the SM as shown in Fig. 1. This is a unique power system configuration and not a realistic one. A real power system is generally meshed, with various SMs, loads and transmission lines.

In [34], for a radial power system, the control scheme calculates the active power that needs to be absorbed to keep the active power of the SM close to its pre-fault value based on the difference between the power passing to the infinite bus through the transmission network during the disturbance and the active power of the SM during pre-fault conditions. The flow chart in Fig. 2 depicts the control scheme.

In this paper, the control scheme [34] was adapted so that it could be successfully implemented in a meshed power system. To this end, the necessary changes to the control scheme are shown in Fig. 3. The flow chart in Fig. 3 depicts the control scheme adapted to operate in a system configuration having multiple transmission lines coming into the PV system's point of common coupling (PCC). The proposed FRT scheme now compensates for the power flows in all the transmission lines coming into the PV system's PCC, the only power flow which is not compensated for is the flow through the transmission line on which there is a fault ($k \neq$ TL-f). The faulted line is identified by a distance relay installed on each transmission line. The meshed configuration adapted power references computation block shown in Fig. 4, depicts how power flow from each transmission line coming

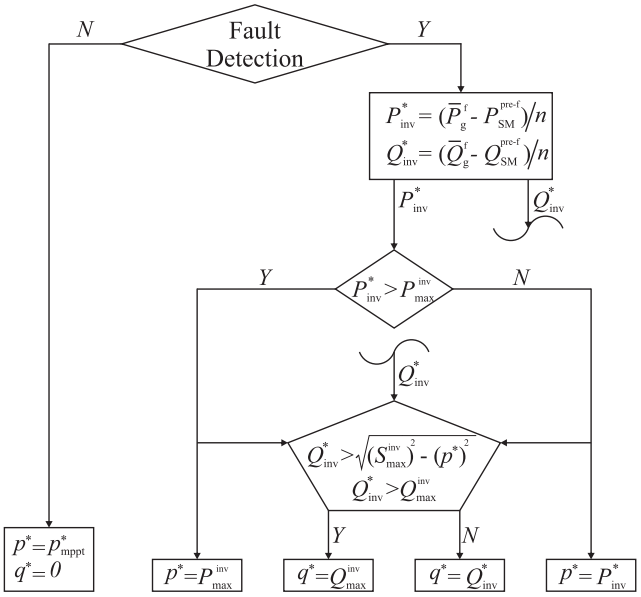

FIGURE 2. Computation of inverter power references based on the control scheme described in [34].

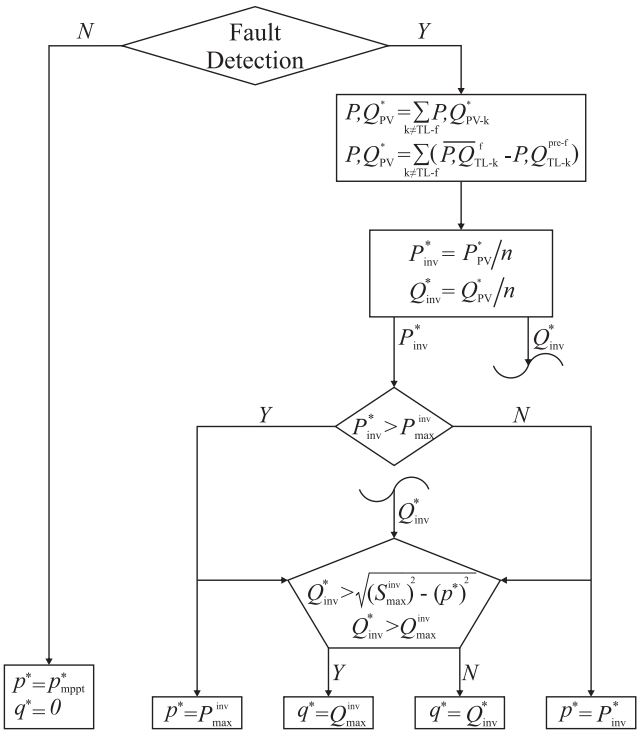

FIGURE 3. Computation of inverter power references adapted for use in a multimachine power system.

into the PCC is compensated for by calculating the inverter power reference needed to keep the power flow in each transmission line at its pre-fault value by absorption of active power into the dc-link capacitors in the PV system. The capacity to absorb is, also, limited by the inverter's maximum dc bus voltage.

A major advantage of a meshed power system is that all the information required for the inverter power reference calculation can be collected at the PCC using measurements from each transmission line's PMU unit installed at the PCC bus, which is also where the PV system's substation is located, resulting in no delay in the transmission of information to the PV system's phasor data concentrator (PDC). This was a setback in [34] because the information regarding the operational status of the SM and grid during the disturbance had to be collected by the PMU unit and transmitted to the PDC located at the PV system substation, causing a delay that could affect the performance of the FRT scheme.

In this work, the information of the operational status from each transmission line is collected by the PMU units and transmitted to a local PDC at a rate of 60 samples/s [37], as shown in Fig. 4. The time-stamped data stream, after being aggregated and compressed by the PDC is fed into an application software to command the PV system's inverters as outlined by the proposed control scheme shown in Fig. 4.

It will be seen in the next sections that the adjustments made to the control scheme presented in [34] allow the scheme to be used in a meshed power system regardless of the position of the fault, effectively supporting the power system by improving transient and voltage stability.

III. THE CHALLENGE OF IMPLEMENTING AN FRT CONTROL SCHEME FOR A PV POWER PLANT IN A MULTIMACHINE POWER SYSTEM

The control scheme in [34] achieved better transient and voltage stability performance than implementation of the control requirements stipulated in the German GC [14]. However, the scheme was not tested in a power system with a meshed configuration with multiple active and reactive power flowing to or from the PCC through transmission lines and multiple SMs with different inertial responses under severe disturbances. The necessary changes to the control scheme in [34] to make it suitable for a PV system connected to a multimachine power system with a meshed transmission network were established in section II.

A power system operating with sources connected to a grid through inverters is subject to existing and new problems related to voltage, frequency and angular stability. These challenges have led to the inclusion of FRT requirements in most GCs, making it necessary for PV system inverters to act during and after fault conditions and to prioritize power system voltage stability by increasing reactive power and reducing or completely stopping the delivery of active power to the system. However, in some cases the PCC short-circuit power may be low, especially after a contingency where the system protection could have tripped an important transmission line, causing the critical voltage identified by the nose point in the power vs. voltage curve to lie within the normal operating voltage range [38].

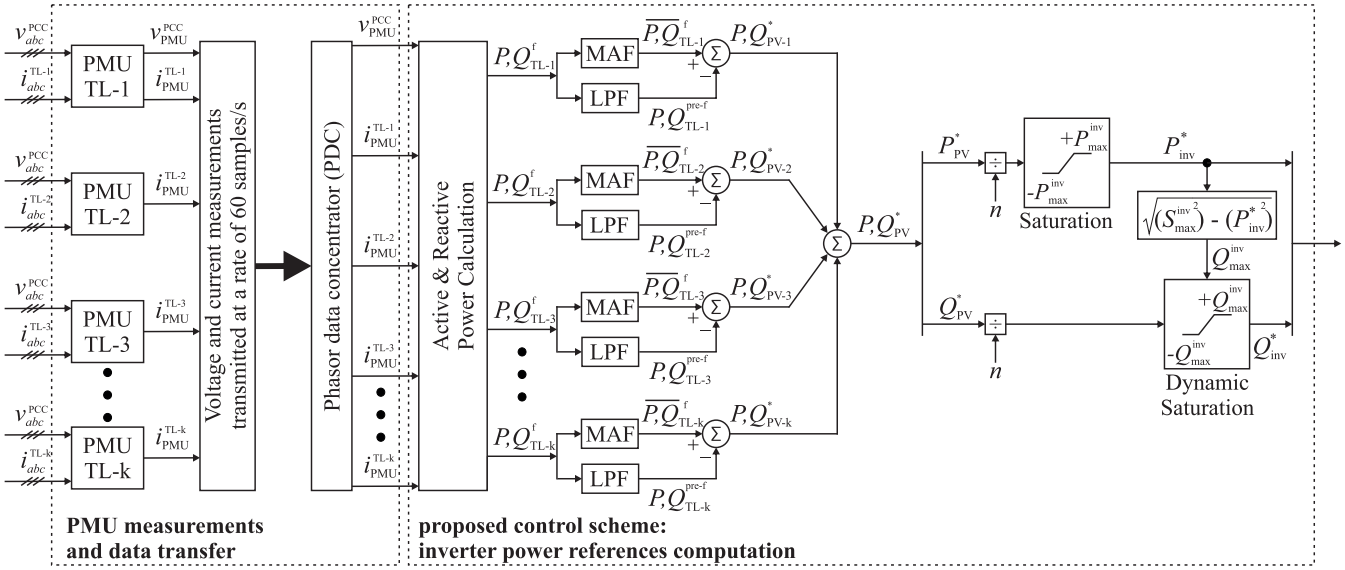

FIGURE 4. Adjustments made to the FRT control scheme [34]: phasor measurement unit (PMU) measurements and data transfer block and FRT inverter power references computation block.

A. STABILITY OF THE WSCC 9-BUS TEST SYSTEM

In the modified WSCC 9-bus test system shown in Fig. 5, a PV system is connected to bus-8, which is considered the PCC. The PV system consisting of twenty-five 2 MW PV units amounts to a total of 50 MVA nominal apparent power (all the technical data for each PV unit can be found in [34]). This amount of power, according to the requirements of most GCs, should be available to be delivered as reactive power during a fault in the transmission system. Power system strength at the PCC is assessed with a contingency (a trip of the power line from bus-7 to bus-8). The reason for choosing this line is that this scenario yields a critical power vs. voltage curve for the PCC bus. The nose curve in Fig. 6 shows that the critical voltage is close to the normal operating range (approximately 0.9 p.u.), which could indicate a potential voltage collapse. From this analysis, any FRT control scheme applied to the inverters of a PV system should be assessed in terms of how well it helps to ensure power system stability.

For this purpose, a three-phase fault located 30 km from bus -7 on the transmission line between buses 7 and 8 is applied. The duration of the fault is 150 ms and the fault is cleared by opening the breakers on the faulted line and closing them with a reclose time of 600 ms. Under these circumstances, the PV system acting as required by the German GC [14] would normally deliver reactive power during the fault, and this should support system voltage stability. However, as can be seen in Fig. 7, when the fault occurs, the voltage drops to 0.15 p.u. even with the inverters' reactive power support during and after the fault, leading to voltage collapse. This fault scenario shows that when the inverter acts according to the requirements established by the German GC, power system stability is not improved. In section IV, the performance of the control scheme in [34] adapted as described in section II will be shown and compared with the results obtained by the control action stipulated by the German GC.

IV. WSCC 9-BUS TEST SYSTEM SIMULATION

The simulation cases were performed using MATLAB/Simulink on the modified WSCC 9-bus test system shown in Fig. 5. The test system is used to illustrate the performance of the proposed PV inverter control scheme adapted for successful operation in a meshed power system with multiple SMs during a contingency on the transmission network. The proposed control scheme aims to balance the power flow going into the PCC, maintaining the active power as close as possible to its pre-fault value by the absorption of active power, which is stored in the PV inverters' dc-link capacitors. Two fault scenarios as shown in Fig. 5 for fault 1 and fault 2, are used to demonstrate the performance of the proposed control scheme:

- The first scenario (case 1) is a three-phase fault located halfway along the transmission line between buses 6 and 9;
- The second scenario (case 2) is also a three-phase fault, this time located three tenths of the way along the transmission line between buses 7 and 8.

Both faults have a duration of 150 ms and the fault is cleared by opening the breakers on the faulted line and closing them with a reclose time of 600 ms.

The next subsections will show the results for both fault scenarios with the proposed control scheme and compare these with the results achieved using the control required by the German GC.

The selection of the FRT requirements established by the German GC for comparison with the proposed control scheme is based on the fact that it has the most stringent

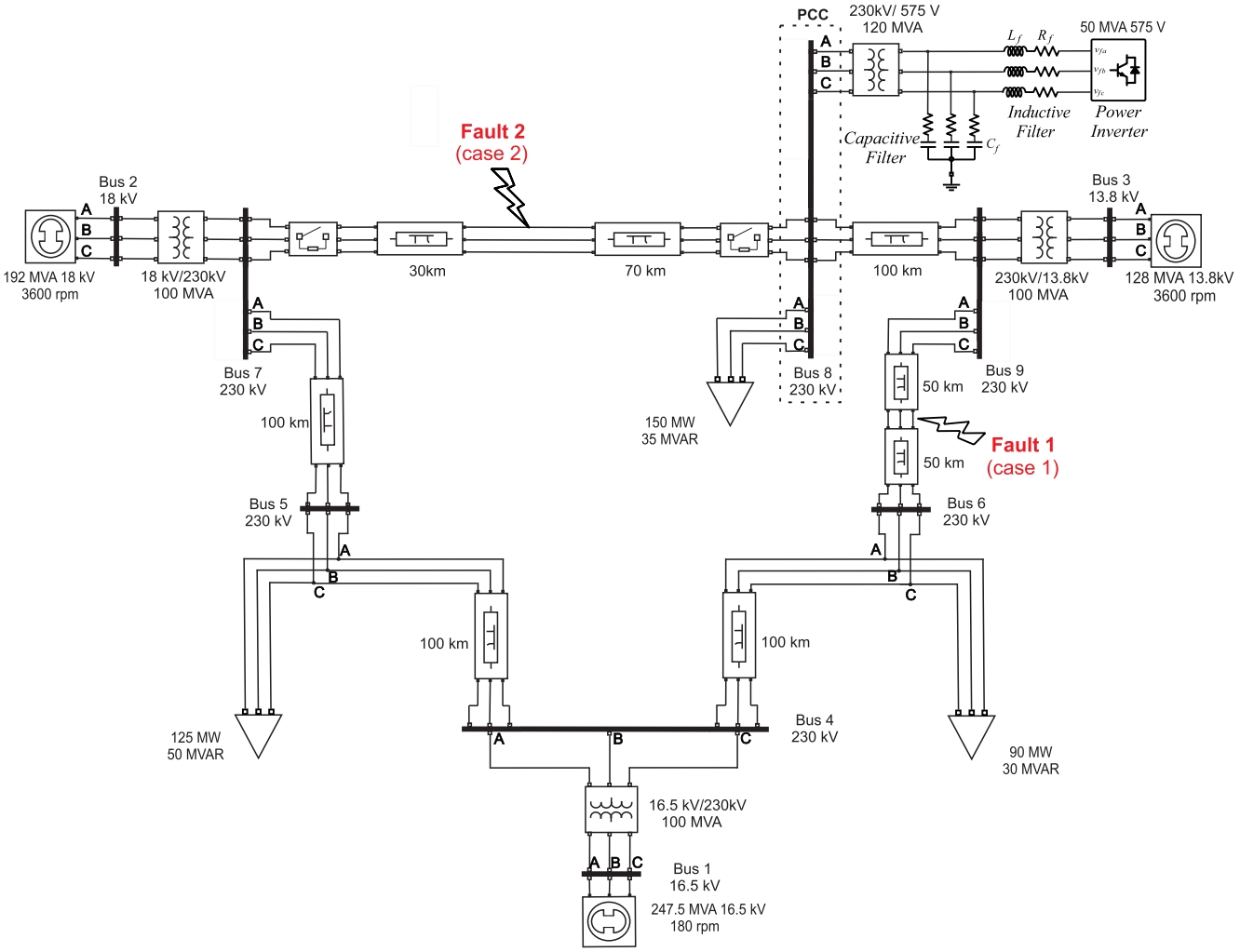

FIGURE 5. Modified WSCC 9-bus system with a PV system connected to bus-8.

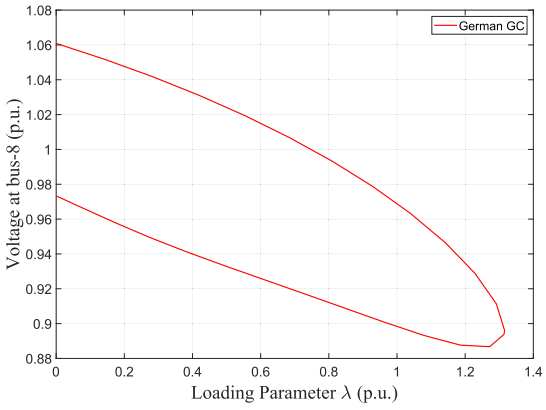

FIGURE 6. Power vs voltage nose curve at bus-8 of the WSCC 9-bus test system.

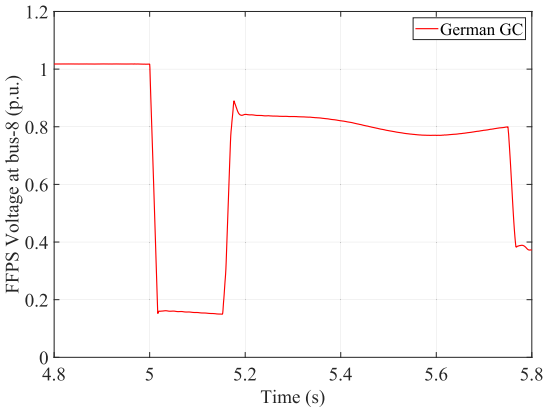

FIGURE 7. Voltage at bus-8 of the WSCC 9-bus test system during and after the fault.

certifications [39], and many FRT control schemes proposed in the literature are compared against the german GC as in [39]–[41]. However, at the end of the results for case 2, a comparison is plotted in Fig. 23 depicting the synchronous machines' rotor angles excursions between the proposed control scheme and some of the most up to date grid codes in operation.

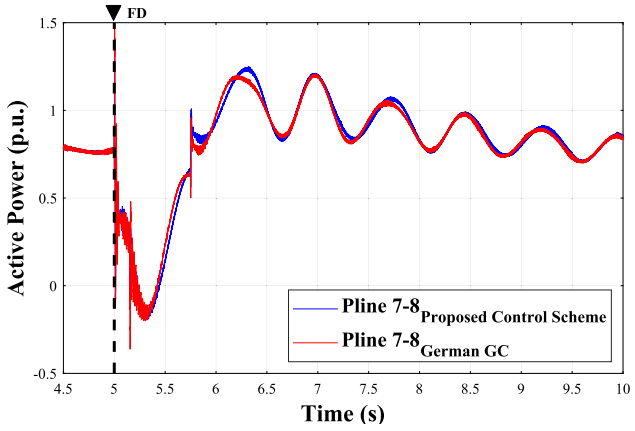

FIGURE 8. Active power flow in the transmission line between buses 7 and 8 in p.u. - case 1.

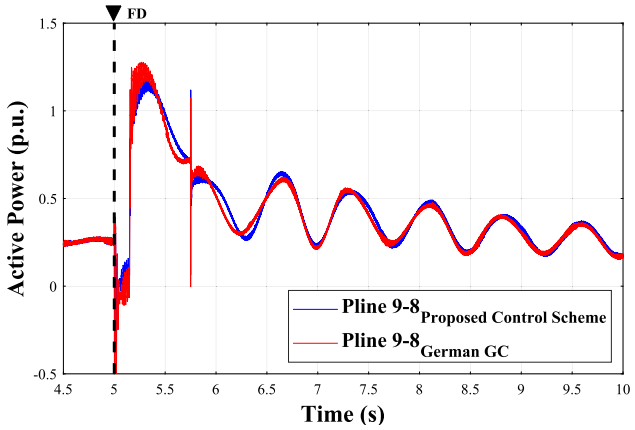

FIGURE 9. Active power flow in the transmission line between buses 8 and 9 in p.u. - case 1.

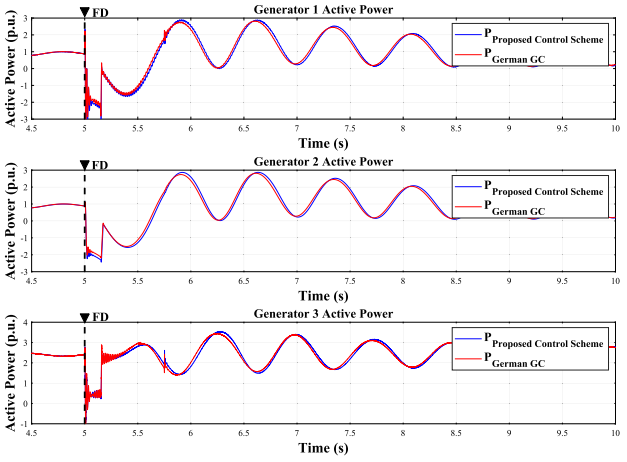

FIGURE 10. Active power output of the test system generators in p.u. - case 1.

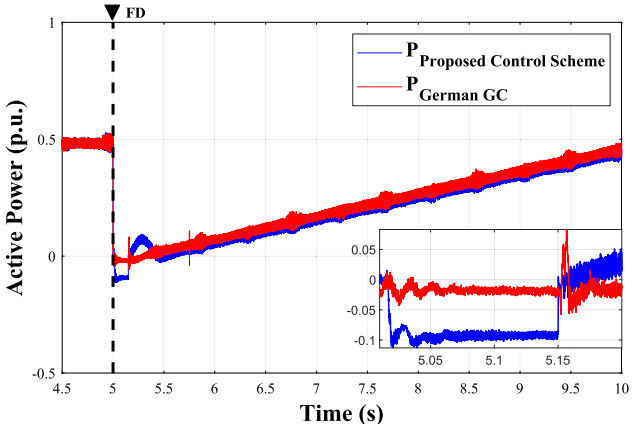

FIGURE 11. Active power output of the test system PV power plant in p.u. - case 1.

A. SIMULATION RESULTS FOR CASE 1

The simulation results in Fig. 8 show a comparison of the active power flow in the transmission line between buses 7 and 8 when the PV inverters act according to the German GC and when the proposed control scheme is used. The responses for both control strategies are very similar, reaching an operating point similar to that before the fault at almost the same time. Fig. 9 shows the active power flow in the transmission line between buses 8 and 9. Although the results for both control strategies are similar, during the fault the active power is slightly higher for the proposed control scheme, confirming the effect of the inverter absorbing active power into the dc-link capacitors.

The active power output of each of the generators is shown in Fig. 10. All the curves for the generators have similar behavior during and after the fault, as would be expected from the previous analysis.

Fig. 11 shows the active power output of the PV system and the fault region in zoom. The active power in this region is negative with the proposed control scheme, indicating that energy is being absorbed, making the slight increase in the power flows in the transmission lines coming into the PCC possible (Figs. 8 and 9). After the fault, both control strategies start to increase the active power output at the Active Power Recovery Ramp Rate (APRRR) of 20%/s established in the German GC.

The reactive power output shown in Fig. 12 illustrates the results of the control action based on the requirements specified in the German GC. Reactive power is delivered to the system as soon as a voltage drop below 0.9 p.u. is detected, as shown in Fig. 13. This is why reactive power support is still being delivered for a short period after the fault has ended. The results for the proposed control scheme indicate that the scheme shown in Fig. 4 calculates that no reactive power support is needed.

In Fig. 13 the results for the PCC voltage show that even with the reactive power support provided by the control strategy based on the German GC, the voltage profile is very similar to that obtained using the proposed control scheme. In this case, voltage stability has been maintained with

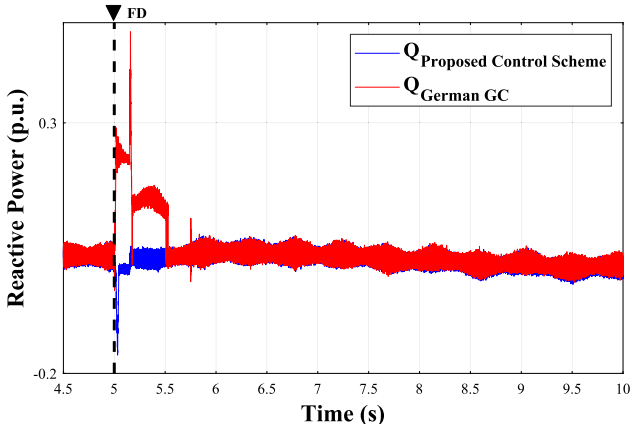

FIGURE 12. Reactive power output of the test system PV power plant in p.u. - case 1.

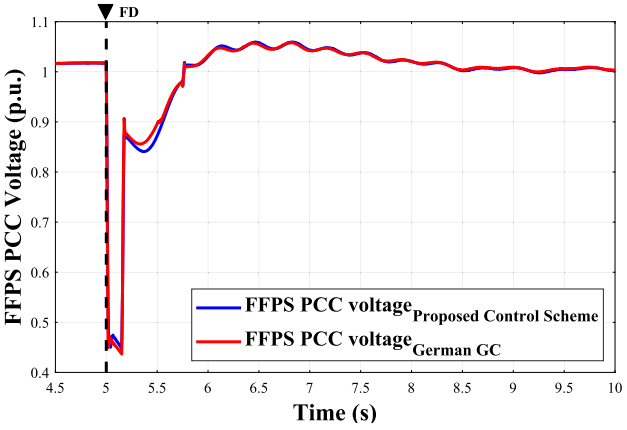

FIGURE 13. Voltage at the PCC in p.u. - case 1.

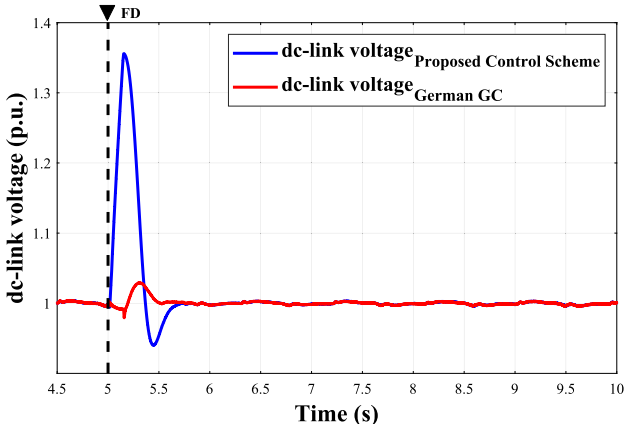

FIGURE 14. Inverter dc-link voltage in p.u. - case 1.

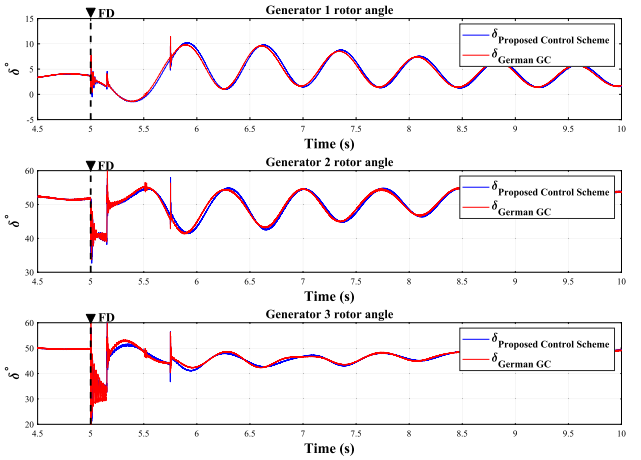

FIGURE 15. SM rotor angle - case 1.

both strategies and there is little difference in performance between them.

Analysis of the dc-link voltage plots in Fig. 14 shows that during the fault the voltage is kept at almost the same value but with small transients when the control strategy based on the German GC is used. In contrast, there is an increase in dc-link voltage during the fault when the proposed control strategy is used. This increase indicates energy is being stored in the inverter's dc-link capacitors; however, this increase is limited by the maximum inverter dc input voltage of 1500 V (1.36 p.u.).

As expected from the previous plots, the rotor angles of all the SMs in the power system shown in Fig. 15 exhibit similar behavior for both control strategies.

Analysis of case 1 indicates that both control strategies have almost the same performance in supporting power system transient and voltage stability. It would seem that no major improvement has been observed with the proposed control strategy. However, this case does not involve a scenario in which the fault location could potentially lead the power system to voltage collapse.

B. SIMULATION RESULTS FOR CASE 2

In subsection III-A it has already been seen that the control response required by the German GC, in which reactive power is delivered from the PV system to the transmission network, can accelerate the loss of power system stability, showing that what is required by most GCs is not always suitable for all contingencies.

The results of the simulation in Fig. 16 show a comparison of the active power flow in the transmission line between buses 8 and 9. (The transmission line between buses 7 and 8 is not shown because the proposed control scheme does not compensate for the faulted line.) When the PV inverters act as required by the German GC, there is a complete loss of stability after the transmission line is reconnected. In contrast, when the proposed control scheme is used the power system remains stable, reaching the pre-fault operating point after approximately 5 s.

The active power output of each of the generators is shown in Fig. 17. As expected from the previous analysis, the inverters using the proposed control scheme keep the generators in synchronism with the power system, whereas

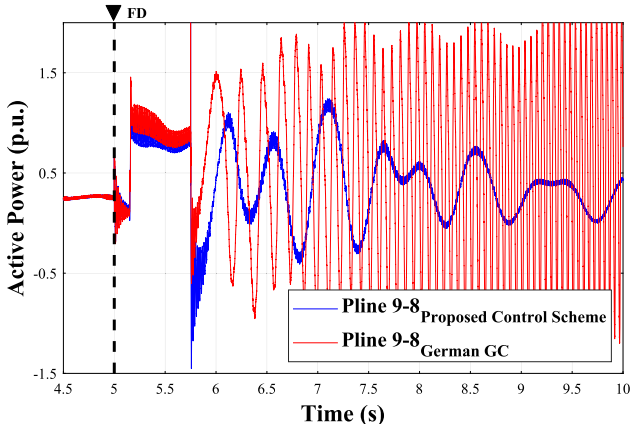

FIGURE 16. Active power flow in the transmission line between buses 8 and 9 in p.u. - case 2.

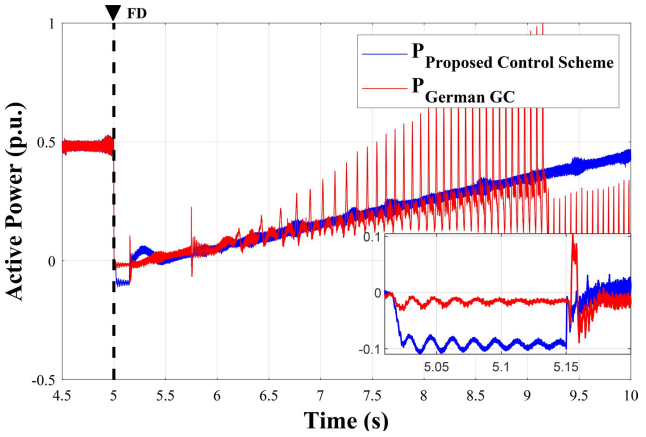

FIGURE 18. Active power output of the test system PV power plant in p.u. - case 2.

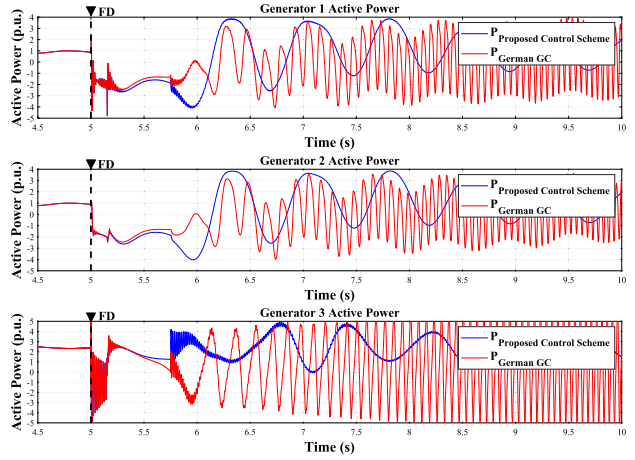

FIGURE 17. Active power output of the test system generators in p.u. - case 2.

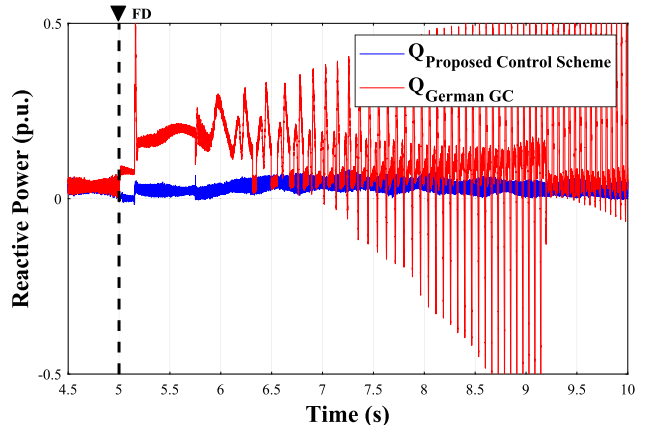

FIGURE 19. Reactive power output of the test system PV power plant in p.u. - case 2.

when the control system based on the German GC is used, synchronism is lost, indicating a loss of power system stability.

The active power output of PV system is shown in Fig. 18. As in case 1, a zoom during the fault period shows negative active power with the proposed control scheme, indicating that energy is being absorbed and making an increase in the power flow in the transmission line coming into the PCC possible (Fig. 16). After the fault, both control strategies start to increase the active power output at the APRRR established in the German GC. However, with control based on the German GC, the system is unable to reach the pre-fault power output because the voltage at the PCC has already collapsed.

The control action required by the German GC makes the inverters deliver reactive power when a voltage drop below 0.9 p.u. is detected, as shown in Fig. 20. However, because the voltage drops to a very low value during the fault (0.15 p.u.), the reactive power output shown in Fig. 19 is very low even though the inverters are injecting reactive current close to their nominal value. Because the voltage is still below 0.9 p.u. after the fault, the inverters continue to inject reactive power, which is not an efficient control action to maintain voltage stability. The voltage at the PCC finally collapses after the transmission line is reconnected. As in case 1, the proposed control scheme calculates that no reactive power support is needed.

In Fig. 20 the results for the PCC voltage show that only the proposed control scheme is able to maintain voltage stability, ensuring that the system returns to an operating point close to pre-fault conditions.

The results for the dc-link voltage in Fig. 21 indicate that the control strategy based on the German GC maintains the voltage at the nominal value of 1100 V. As in case 1, an increase in dc-link voltage during the fault with the proposed control strategy is expected as energy is being stored in the inverters' dc-link capacitors. However, this increase does not exceed the maximum inverter dc input voltage of 1500 V (1.36 p.u.).

As expected given the behavior of the active power outputs of the SMs, the rotor angles of all the SMs in the power system shown in Fig. 22 oscillate less when the proposed

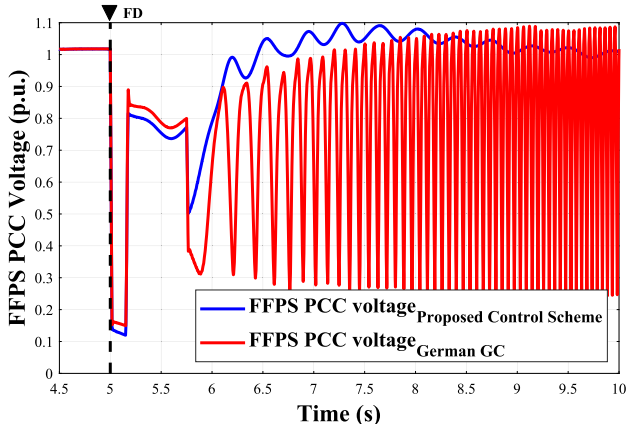

FIGURE 20. Voltage at the PCC in p.u. - case 2.

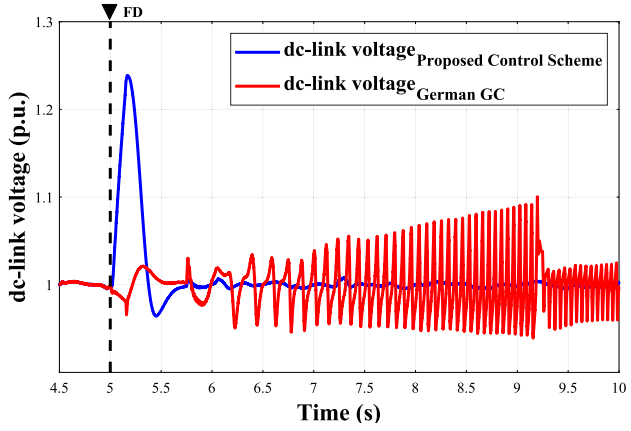

FIGURE 21. Inverter dc-link voltage in p.u. - case 2.

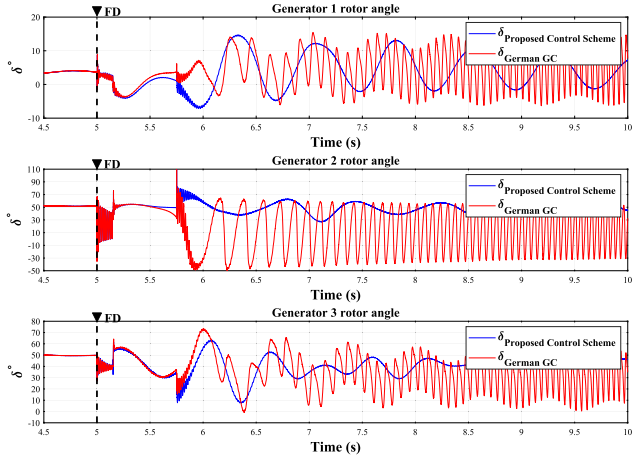

FIGURE 22. SM rotor angle - case 2.

control scheme is implemented, ensuring transient stability. The control action required by the German GC nor by any of the other GCs illustrated in Fig. 23 are not able to reduce the oscillations of the rotor angles of the SMs, leading to a loss of transient stability.

The results for the proposed control scheme prove its effectiveness in maintaining power system stability.

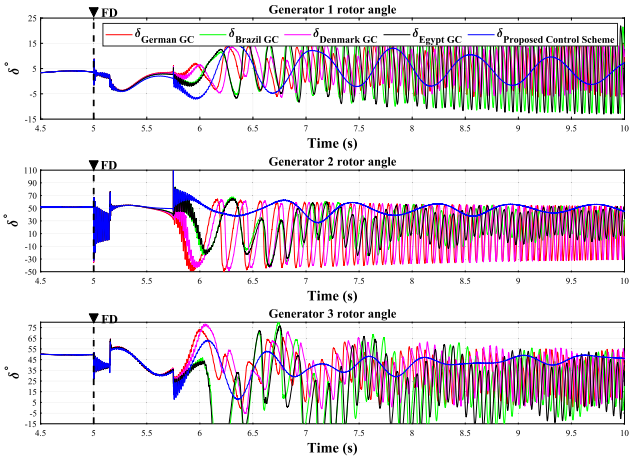

FIGURE 23. SM rotor angle responses with the proposed control scheme compared with various GCs - case 2.

By giving priority to the absorption of active power instead of the reactive power support required by most GCs, the proposed control scheme has been shown to be able to solve two major stability problems: transient and voltage stability in power systems with PV resources connected to the grid through inverters for any contingency scenario.

V. CONCLUSION

In this work, the control scheme for PV inverters presented in [34] has been adapted for use during severe disturbances in the transmission network of a meshed power system with multiple SMs.

The control scheme priority of improving transient stability rather than voltage stability resulted in better performance than the control action required by the German GC and with other GCs in power systems with a voltage condition that could lead to voltage collapse. In such a case, reactive power support may even accelerate voltage collapse.

The simulation results with the proposed control scheme show that the rotor angles of the SMs return to their pre-fault operating values and, even without reactive power, the voltages on all the buses in the power system are restored to their pre-fault values as well.

The analysis presented here has shown that the proposed control scheme can be implemented in the inverters of a PV system to improve the transient and voltage stability of a multimachine power system.

REFERENCES

[1] J. P. Viteri, F. Henao, J. Cherni, and I. Dyner, "Optimizing the insertion of renewable energy in the off-grid regions of Colombia," *J. Cleaner Prod.*, vol. 235, pp. 535–548, Oct. 2019.
[2] B. Dhinesh and M. Annamalai, "A study on performance, combustion and emission behaviour of diesel engine powered by novel nano nerium oleander biofuel," *J. Cleaner Prod.*, vol. 196, pp. 74–83, Sep. 2018.
[3] A. Giallanza, M. Porretto, G. L. Puma, and G. Marannano, "A sizing approach for stand-alone hybrid photovoltaic-wind-battery systems: A sicilian case study," *J. Cleaner Prod.*, vol. 199, pp. 817–830, Oct. 2018.
[4] F. Obeidat, "A comprehensive review of future photovoltaic systems," *Sol. Energy*, vol. 163, pp. 545–551, Mar. 2018.

[5] H. M. Hasanien, "An adaptive control strategy for low voltage ride through capability enhancement of grid-connected photovoltaic power plants," *IEEE Trans. Power Syst.*, vol. 31, no. 4, pp. 3230–3237, Jul. 2016.

[6] A. Honrubia-Escribano, F. J. Ramirez, E. Gómez-Lázaro, P. M. Garcia-Villaverde, M. J. Ruiz-Ortega, and G. Parra-Requena, "Influence of solar technology in the economic performance of PV power plants in Europe. A comprehensive analysis," *Renew. Sustain. Energy Rev.*, vol. 82, pp. 488–501, Feb. 2018.

[7] H. Kobayashi, "Fault ride through requirements and measures of distributed PV systems in Japan," in *Proc. IEEE Power Energy Soc. Gen. Meeting*, Jul. 2012, pp. 1–6.

[8] *Requisitos de Respuesta Frente a Huecos de Tensión de Las Instalaciones Eólicas*, Secretaría General de Energía P.O. 12.3, Madrid, Spain, Oct. 2006.

[9] *Instalaciones Conectadas a la Red de Transporte y Equipo Generador: Requisitos Mínimos de Diseño, Equipamiento, Funcionamiento, Puesta en Servicio y Seguridad, Draft Version*, Red eléctrica Española P.O. 12.2, Madrid, Spain, Sep. 2010.

[10] H. Berndt, M. Hermann, H. D. Kreye, R. Reinisch, U. Scherer, and J. Vanzetta, *Network and System Rules of the German Transmission System Operators*. Berlin, Germany: Transmission Code, 2007.

[11] M. R. Islam, H. Lu, M. J. Hossain, and L. Li, "Mitigating unbalance using distributed network reconfiguration techniques in distributed power generation grids with services for electric vehicles: A review," *J. Cleaner Prod.*, vol. 239, Dec. 2019, Art. no. 117932.

[12] A. Q. Al-Shetwi, M. Z. Sujod, and N. L. Ramli, "A review of the fault ride through requirements in different grid codes concerning penetration of pv system to the electric power network," *ARPN J. Eng. Appl. Sci.*, vol. 10, no. 21, pp. 9906–9912, 2015.

[13] W. Bartels, F. Ehlers, K. Heidenreich, R. Huttner, H. Kuhn, T. Meyer, T. Kumm, J. Salzmann, H. Schafer, and K. Weck, "Generating plants connected to the medium-voltage network," in *Proc. Tech. Guideline BDEW*. Berlin, Germany, Jun. 2008, pp. 1–130.

[14] *Technical Requirements for the Connection and Operation of Costumer Installations to the High-Voltage Network (TCC High-Voltage)*, document VDE-AR-N 4120, Jan. 2015.

[15] CEI, Comitato Elettrotecnico Italiano. (2016). *Reference Technical Rules for the Connection of Active and Passive Consumers to the HV and MV Electrical Networks of Distribution Company*. Accessed: Apr. 14, 2020. [Online]. Available: http://www.ceiweb.it/

[16] *IEEE Standard for Interconnecting Distributed Resources With Electric Power Systems*, Standard 1547-2003, 2003.

[17] *IEEE Standard for Interconnection and Interoperability of Distributed Energy Resources With Associated Electric Power Systems Interfaces*, Standard 1547-2018, Apr. 2018.

[18] *National Electricity Rules Version 63*, AEMC, Chennai, India, 2014.

[19] D. Energinet, "Technical regulation 3.2.2 for PV power plants above 11 kw," KDJ, Energinet, Fredericia, Denmark, Tech. Rep., 2015.

[20] *Technical Requirements for Connecting Photovoltaic Power Station to Power System*, document Chinese Grid Code GB/T 19964-2012, Jun. 2013.

[21] *EirGrid Grid Code Version 6.0*, EirGrid, Dublin, Ireland, 2015.

[22] *Photovoltaic (PV) Systems—Characteristics of the Utility Interface*, document IEC 61727, International Electrotechnical Commission, IEC, London, U.K., 2004.

[23] A. Anzalchi and A. Sarwat, "Overview of technical specifications for grid-connected photovoltaic systems," *Energy Convers. Manage.*, vol. 152, pp. 312–327, Nov. 2017.

[24] S. S. Rangarajan, E. R. Collins, J. C. Fox, and D. P. Kothari, "A survey on global PV interconnection standards," in *Proc. IEEE Power Energy Conf. at Illinois (PECI)*, Feb. 2017, pp. 1–8.

[25] M. Mohseni and S. M. Islam, "Review of international grid codes for wind power integration: Diversity, technology and a case for global standard," *Renew. Sustain. Energy Rev.*, vol. 16, no. 6, pp. 3876–3890, 2012.

[26] E. M. G. Rodrigues, G. J. Osório, R. Godina, A. W. Bizuayehu, J. M. Lujano-Rojas, and J. P. S. Catalão, "Grid code reinforcements for deeper renewable generation in insular energy systems," *Renew. Sustain. Energy Rev.*, vol. 53, pp. 163–177, Jan. 2016.

[27] T. Dragicevic, X. Lu, J. C. Vasquez, and J. M. Guerrero, "DC microgrids—Part II: A review of power architectures, applications, and standardization issues," *IEEE Trans. Power Electron.*, vol. 31, no. 5, pp. 3528–3549, May 2016.

[28] A. Brem, M. M. Adrita, D. T. J. O'Sullivan, and K. Bruton, "Industrial smart and micro grid systems—A systematic mapping study," *J. Cleaner Prod.*, vol. 244, Jan. 2020, Art. no. 118828.

[29] M. Tsili and S. Papathanassiou, "A review of grid code technical requirements for wind farms," *IET Renew. Power Generat.*, vol. 3, no. 3, pp. 308–332, Sep. 2009.

[30] R. Shah, N. Mithulananthan, R. C. Bansal, and V. K. Ramachandaramurthy, "A review of key power system stability challenges for large-scale PV integration," *Renew. Sustain. Energy Rev.*, vol. 41, pp. 1423–1436, Jan. 2015.

[31] K. Loudiyi, A. Berrada, H. G. Svendsen, and K. Mentesidi, "Grid code status for wind farms interconnection in Northern Africa and Spain: descriptions and recommendations for northern Africa," *Renew. Sustain. Energy Rev.*, vol. 81, pp. 2584–2598, Jan. 2018.

[32] A. Cabrera-Tobar, E. Bullich-Massagué, M. Aragüés-Peñalba, and O. Gomis-Bellmunt, "Review of advanced grid requirements for the integration of large scale photovoltaic power plants in the transmission system," *Renew. Sustain. Energy Rev.*, vol. 62, pp. 971–987, Sep. 2016.

[33] A. Fernández-Guillamón, E. Gómez-Lázaro, E. Muljadi, and Á. Molina-García, "Power systems with high renewable energy sources: A review of inertia and frequency control strategies over time," *Renew. Sustain. Energy Rev.*, vol. 115, Nov. 2019, Art. no. 109369.

[34] O. C. Zevallos, J. B. Da Silva, F. Mancilla-David, F. A. Neves, R. C. Neto, and R. B. Prada, "Control of photovoltaic inverters for transient and voltage stability enhancement," *IEEE Access*, vol. 9, pp. 44363–44373, 2021.

[35] A. Delavari and I. Kamwa. *WSCC 9-Bus Test System IEEE Benchmark. MATLAB Central File Exchange*. Accessed: Jan. 20, 2022. [Online]. Available: https://in.mathworks.com/matlabcentral/fileexchange/45936-ieee-9-bus

[36] ABB Central Inverters. *PVS980-58 Central Inverters Hardware Manual*. Accessed: Jan. 20, 2022. [Online]. Available: https://new.abb.com/news/detail/23761/abb-launches-next-generation-central-i%nverter-with-unique-cooling-capabilities

[37] G. Dileep, "A survey on smart grid technologies and applications," *Renew. Energy*, vol. 146, pp. 2589–2625, Feb. 2020.

[38] J. Matevosyan, J. MacDowell, N. Miller, B. Badrzadeh, D. Ramasubramanian, A. Isaacs, R. Quint, E. Quitmann, R. Pfeiffer, H. Urdal, T. Prevost, V. Vittal, D. Woodford, S. H. Huang, and J. O'Sullivan, "A future with inverter-based resources: Finding strength from traditional weakness," *IEEE Power Energy Mag.*, vol. 19, no. 6, pp. 18–28, Nov. 2021.

[39] Y. Bae, T.-K. Vu, and R.-Y. Kim, "Implemental control strategy for grid stabilization of grid-connected PV system based on German grid code in symmetrical low-to-medium voltage network," *IEEE Trans. Energy Convers.*, vol. 28, no. 3, pp. 619–631, Sep. 2013.

[40] P. Piya, M. Ebrahimi, M. Karimi-Ghartemani, and S. A. Khajehoddin, "Fault ride-through capability of voltage-controlled inverters," *IEEE Trans. Ind. Electron.*, vol. 65, no. 10, pp. 7933–7943, Oct. 2018.

[41] G. Lammert, J. C. Boemer, D. Premm, O. Glitza, L. D. P. Ospina, D. Fetzer, and M. Braun, "Impact of fault ride-through and dynamic reactive power support of photovoltaic systems on short-term voltage stability," in *Proc. IEEE Manchester PowerTech*, Jun. 2017, pp. 1–6.

YANDI G. LANDERA was born in Cuba, in 1986. He received the B.S. and M.Sc. degrees in electrical engineering from the Central University of Las Villas, Santa Clara, Cuba, in 2010 and 2012, respectively. He is currently pursuing the Ph.D. degree in electrical engineering with the Federal University of Pernambuco, Recife, Brazil.

In 2016 and 2018, he was a part of the fellowship program offered by the International Sustainable Energy Development Center and the National Institute of Solar Energy in Russia and India, respectively. Since 2018, he has been with the Power Electronics and Electric Drive Group, Federal University of Pernambuco. His research interests include voltage and transient stability, power electronics, renewable energy integration, and grid-connected converters.

OSCAR C. ZEVALLOS (Member, IEEE) was born in Cusco, Perú, in 1985. He received the B.S. degree in electrical engineering from the Universidad Nacional de San Antonio Abad del Cusco, Cusco, in 2010, and the M.S. and Ph.D. degrees in electrical engineering from the Pontifical Catholic University of Rio de Janeiro, Brazil, in 2014 and 2020, respectively.

Since 2020, he has been a Postdoctoral Researcher with the Pontifical Catholic University of Rio de Janeiro. His research interests include voltage and transient stability, power electronics, renewable energy integration, and control of converters.

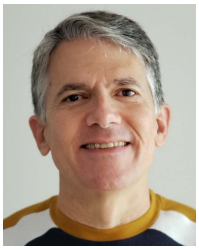

FRANCISCO A. S. NEVES (Senior Member, IEEE) was born in Campina Grande, Brazil, in 1963. He received the B.S. and M.Sc. degrees in electrical engineering from the Universidade Federal de Pernambuco, Recife, Brazil, in 1984 and 1992, respectively, and the Ph.D. degree in electrical engineering from the Universidade Federal de Minas Gerais, Belo Horizonte, Brazil, in 1999.

Since 1993, he has been with the Department of Electrical Engineering, Universidade Federal de Pernambuco, where he is currently a Full Professor. He was a Visiting Scholar with the Georgia Institute of Technology, Atlanta, GA, USA, in 1999; and the University of Alcala, Madrid, Spain, from 2008 to 2009. His research interests include power electronics, renewable energy systems, power quality, and grid-connected converters.

RAFAEL C. NETO (Student Member, IEEE) was born in Cabo de Santo Agostinho, Brazil, in 1991. He received the B.S. degree in electronic engineering and the M.Sc. and D.Sc. degrees in electrical engineering from the Universidade Federal de Pernambuco, Recife, Brazil, in 2016, 2018, and 2020, respectively.

He was a Visiting Scholar with the Universidade Federal de Santa Maria, Brazil, in 2016. Since 2020, he has been with the Department of Electrical Engineering, Universidade Federal de Pernambuco. His research interests include power electronics, renewable energy systems, and modeling and digital control techniques of static converters.

RICARDO B. PRADA was born in 1951. He received the Diploma degree in electrical engineering and the M.Sc. degree in power systems from the Pontifical Catholic University of Rio de Janeiro, Rio de Janeiro, Brazil, in 1975 and 1977, respectively, and the Ph.D. degree in electrical engineering from the Imperial College of Science and Technology, London, U.K., in 1980. He is currently an Associate Professor with the Department of Electrical Engineering, Pontifical Catholic University of Rio de Janeiro.